ANTIOXIDANTS & REDOX SIGNALING
Volume 10, Number 12, 2008

DOI: 10.1089/ars.2007.1876

Original Research Communication

Triglycerides Potentiate the Inflammatory Response in Rat Kupffer Cells

Noga Budick-Harmelin,[1] Jozsef Dudas,[2] Julia Demuth,[2] Zecharia Madar,[1]
Giuliano Ramadori,[2] and Oren Tirosh[1]

Abstract

Accumulation of fat in the liver, also known as steatosis, may lead to inflammation and tissue damage. Kupffer cells (KCs) are the resident macrophages of the liver and have an important role in inflammatory reactions. The inflammatory response of isolated rat KCs to endotoxin in the presence of lipids was investigated in this study. KCs were treated with lipopolysaccharide (LPS) and triglycerides (TGs) alone or in combination. TGs had no effect on the expression of pro-inflammatory mediators, but adding TGs to LPS enhanced the induction of inducible nitric oxide synthase (iNOS), tumor necrosis factor-α (TNF-α), interleukin-1β (IL-1β), interleukin-6 (IL-6), and granulocyte colony-stimulating factor (G-CSF), compared with LPS treatment alone. Increased DNA binding of NF-κB transcription factor was seen on simultaneous exposure of the cells to TGs and LPS, which was accompanied by decreased intracellular ROS production and increased GSH levels. The inflammation-potentiating effect of TGs on iNOS expression was abolished on NF-κB inhibition. This enhanced inflammatory response might indicate a contribution of lipids to the inflammatory conditions in the fatty liver by increased activation of KCs. *Antioxid. Redox Signal*. 11, 2009–2022.

Introduction

Fat accumulation in nonadipose tissues is a prominent outcome of overnutrition and obesity. Over time, this lipid overload might be associated with tissue damage and organ dysfunction (43). Nonalcoholic fatty liver disease (NAFLD) is a medical condition in which the liver is invaded with fat and excessive amounts of lipids are present within hepatocytes, a morbidity known as steatosis. Fatty liver is the hepatic manifestation of the metabolic syndrome, a growing problem in the modern Western world, characterized by insulin resistance, obesity, elevated blood lipids levels, and high blood-pressure values (7, 49).

NAFLD might worsen into a more serious condition, known as nonalcoholic steatohepatitis (NASH), in which fat accumulation is accompanied by an inflammatory process in the liver. NASH might eventually lead to fibrosis and severe cirrhosis in some patients. The development of liver inflammation is a crucial rate-limiting step in the progression of NAFLD and might play a detrimental role in long-term prognosis (49). The inflammatory process may be initiated by liver resident cells and by recruited inflammatory cells (38). The pathomechanism dictating development of inflammation and transition from NAFLD to NASH is not fully understood and may involve different liver cell populations.

Kupffer cells (KCs) are the resident macrophages of the liver, located mainly in the lumen of the hepatic sinusoids (2) and represent the largest population of tissue macrophages in the body (5). Besides participation in homeostatic responses, KCs play essential roles in host defense by constantly contacting the portal blood entering the liver. In addition to phagocytosis of particulate material, involvement of KCs in immunologic and inflammatory reactions has been suggested (2, 3, 38). Activation of KCs, like other macrophages, is strongly induced by the bacterial endotoxin lipopolysaccharide (LPS), which might originate from gram-negative bacteria found in the gastrointestinal (GI) tract. This process is associated with increased production and release

[1]The School of Nutritional Sciences, Institute of Biochemistry, Food Science and Nutrition, Faculty of Agricultural, Food and Environmental Quality Sciences, The Hebrew University of Jerusalem, Israel.
[2]Department of Internal Medicine, Section of Gastroenterology and Endocrinology, Georg-August-University Göettingen, Germany.

of inflammatory mediators, nitric oxide (NO), cytokines, and reactive oxygen species (ROS) by the cells (5).

NO is a key player in various hepatic pathologies, released by different cell types and generated in KCs as an outcome of strong activation of inducible nitric oxide synthase (iNOS) under inflammatory conditions (30). During endotoxemia, released NO is involved in modulation of the immune response (13). Pro-inflammatory cytokines released by activated KCs, including TNF-α, IL-6, and IL-1, are important regulators of the response during inflammatory activation (2, 38, 48). Likewise, granulocyte colony-stimulating factor (G-CSF) is produced by macrophages on LPS stimulation. G-CSF can modulate the function of immune cells, and local production of G-CSF serves as recruiting signal for neutrophils into the inflammatory foci during infection (23). Toll-like receptor 4 (TLR4), the transmembrane receptor specific for LPS, acts together with CD14, a key mediator in the LPS-signaling pathway in KCs (5, 48). This signal cascade results in activation of the transcription factor nuclear factor-κB (NF-κB) and induction of pro-inflammatory mediator production (48). Proper control over this activation is crucial to avoid exaggerated response and deterioration of pathophysiologic conditions (19).

Lipids can alter the immune cells function and responses. *In vitro* and *in vivo* studies of macrophages showed that exposure to various lipids exhibits a variety of influences over NO production, ROS generation, cytokine-release profile, adhesion ability, phagocytic activity, and cell viability (4, 8, 12, 16). We hypothesized that increased TGs accumulation in the liver may stimulate inflammatory response by hepatic KCs. In this study, KCs were briefly exposed simultaneously to TGs and endotoxin. The study aimed to analyze the effect of TGs on the inflammatory activation of KCs, a mechanism in which lipid-exposed KCs may be involved in the production of inflammatory mediators.

Materials and Methods

Animals

Male Sprague–Dawley rats with a body weight of 400 to 500 g were purchased from Harlan–Winkelmann (Borchen, Germany) and kept under standard conditions with 12-h light/dark cycles and free access to food and water. All procedures were performed in accordance with the institution's guidelines, the German Convention for Protection of Animals, and the National Institutes of Health guidelines.

Materials

The materials used were obtained as follows: Pentobarbital sodium (Narcoren; Merial, Hallbergmoos, Germany); Media M199 (Biochrom, Berlin, Germany); Nycodenz (Axisshield, Oslo, Norway); Agarose, Alexa-labeled secondary antibodies, HEPES buffer, L-glutamine, MMLV Reverse Transcriptase, dNTPs, Platinum SYBR Green qPCR SuperMix-UDG (Invitrogen, Carlsbad, CA); penicillin-streptomycin (Cambrex, Carlskoga, Sweden); FCS (PAA, Linz, Austria); Pronase E (Merck, Darmstadt, Germany); BSA (Serva, Heidelberg, Germany); DNase I (Roche Diagnostics GmbH, Mannheim, Germany); lipid emulsion (Lipofundin 20% containing 5% 16:0; 2% 18:0; 12% 18:1; 27% 18:2; 4% 18:3 and 50% medium-chain fatty acids) (B. Braun, Melsungen, Germany); long-chain triglycerides emulsion (ClinOleic emulsion 20% containing 13.5% 16:0; 2.9% 18:0; 59.5% 18:1; 18.5% 18:2 and 2% 18:3 fatty acids) (Baxter, Unterschleissheim, Germany); antibody for NF-κB p65 (sc-8008), antibody for TLR4 (sc-30002), antibody for CD14 (sc-5749), antibody for MyD88 (sc-8196) (Santa Cruz Biotechnologies, Santa Cruz, CA); antibody for iNOS (BD Transduction Laboratories, Erembodegem, Belgium); mouse negative control for immunocytochemistry, anti-mouse (HRP labeled) antibody, anti-goat (HRP labeled) antibody, anti-rabbit (HRP or biotin labeled) antibodies (DAKO, Glostrup, Denmark); streptavidin (HRP labeled) (Southern Biotech, Birmingham, AL); oligo $(dT)_{15}$, ECL Western blotting detection reagents, x-ray film for EMSA (Amersham, Buckinghamshire, U.K.); x-ray film for Western blot (Konica, Munich, Germany); Bradford reagent (Pierce, Rockford, IL); primary antibody for ED2 (CD163) (Serotec, Düsseldorf, Germany); DAPI (Molecular Probes, Leiden, The Netherlands); T4 Polynucleotide Kinase, Kinase 10X Reaction Buffer, NF-κB Consensus Oligonucleotide (Promega, Madison, WI); collagenase, lipopolysaccharide (LPS) from *Salmonella minnesota*, Nile red, Paraoxon, palmitic acid, linoleic acid, Zymosan from *Saccharomyces cerevisiae*, acrylamide, Triton X-100, primary antibody for β-actin, EDTA, DTT, PMSF, NP-40 (Igepal), Bay 11-7082 (Sigma, Steinheim, Germany); blocking reagent for Western blot (Applichem, Darmstadt, Germany).

Isolation of KCs from rat liver

KCs were isolated according to the method of Knook *et al.* (29), as described elsewhere (2) with some modifications. In brief, after anesthesia, the rat liver was first perfused with 100 ml Gay's balanced salt solution (GBSS) and then digested by perfusion with pronase and pronase/collagenase solutions. The liver was then removed and stirred in 200 ml pronase/collagenase/DNase-solution on a magnetic stirrer at 37°C for 40 min while the pH was kept between 7.4 and 7.5. The obtained cells were passed through a 12-mm cell sieve. The hepatocytes were removed by differential centrifugation, and the remaining nonparenchymal cells, were collected and mixed with a Nycodenz solution to a final concentration of 17.5 g/dl. The density-gradient centrifugation was performed at 1,400 *g* for 17 min. Thereafter, the interphase was collected, and KCs were separated from other cells according to size by counterflow elutriation by using a Beckman centrifuge (J 2-21, JE-6B rotor; Beckman Instruments, Munich, Germany). The rotor speed was 2,500 rpm, and the KCs fraction was collected at a flow rate of 55 ml/min. The obtained KCs were sedimented, resuspended in culture medium (M199 supplemented with 15% FCS, 1% L-glutamine, 100 U/ml penicillin, and 100 μg/ml streptomycin) and counted in a Neubauer chamber after trypan blue staining. Cells were then plated onto six-well plates (500,000 cells/ml), and cultures were kept at 37°C in a humidified atmosphere containing 95% air and 5% CO_2.

Immunocytochemistry and culture purity

KCs were plated onto eight-chamber (Lab-tek) slides (Nunc, Roskilde, Denmark), and medium was replaced 16–18 h after plating. Twelve hours later, cultures were

washed with phosphate-buffered saline (PBS), pH 7.4, and fixed with methanol (−20°C for 10 min) and acetone (−20°C for 10 sec). Then the slides were air-dried and stored at −20°C until further use. Immunocytochemistry was performed by using an immunofluorescence technique. After washing with PBS, pH 7.4, cells were covered with FCS/BSA solution for 1 h, washed again, and then incubated with antibody against ED2 (CD163) (1:150 dilution in PBS) at 4°C overnight. Then the cells were washed 3 times with PBS and incubated with secondary Alexa 555-labeled antibody (1:400 dilution in PBS) at room temperature for 1 h. Counterstaining of the nuclei was done by using 4′,6-diamidino-2-phenylindole, dihydrochloride (DAPI), and the cells were examined with fluorescence microscopy (Axiovert 200 with apotome function; Zeiss, Göttingen, Germany). To verify specific binding, mouse negative control serum was used as a staining control instead of the first antibody, representing the same immunoglobulin class of the relevant antibody.

Treatment with LPS, lipid emulsions, and free fatty acids

Sixteen to 18 h after plating and 6 h before treatment of the cells, culture medium was replaced. LPS (3 μg/ml), Zymosan (3 μg/ml), Lipofundin lipid emulsion (LE), ClinOleic long-chain triglycerides (LCTs) emulsion (to a final concentration of 0.1% TGs), or free fatty acids (FFAs; to a final concentration of 10 or 100 μM) were added to the culture media in the plates for 2 and 6 h, as indicated. Cells were then washed 3 times with PBS, pH 7.4, and RNA samples, total cell protein samples, or nuclear extract samples were collected.

In some experiments, the I-κB phosphorylation inhibitor, Bay 11-7082, was added to the culture media (to a concentration of 1 μM) 1 h before treatment.

Thin-layer chromatography

Culture medium samples were collected from control cells and from cells treated with LE for 6 h. Samples were analyzed relative to LE and to TGs and FFAs standards on a silica gel plate (Merck, Darmstadt, Germany). The solvent system comprised petrol ether, diethyl ether, and acetic acid in a volumetric ratio of 80:19:1. Visualization of the compounds on the plates was performed with iodine staining.

Nile red staining for detection of intracellular lipid accumulation

KCs were seeded onto six-well plates (500,000 cells/ml), and fresh medium was added 16–18 h after plating. Six hours later, cells were exposed to LPS and/or LE (0.1% TGs), which were added to the culture medium for up to 12 h. Nile red staining was performed as it was described by Fowler *et al.* (20), with some modifications. For this staining, stock dye solution was prepared by dissolving Nile red powder in acetone (0.5 μg/ml) and was stored protected from light at 4°C. Before staining, cells were fixated for 15 min by using 4% formaldehyde freshly prepared from paraformaldehyde. Fresh staining solution was made by diluting the stock solution in 75% glycerol (2 μl/ml) and applied to the fixated cells. After 5 min, the cultures were examined with fluorescence microscopy.

Total RNA isolation and gene-expression analysis with quantitative real-time RT-PCR

Total RNA was isolated from the cells by using Trizol according to the instructions of the manufacturer. cDNA was generated by reverse transcription of 2 μg of total RNA by using primer oligo $(dT)_{15}$. The expression level of mRNA was quantified with real-time PCR by using Sybr Green qPCR mix in an ABI Prism 7000 sequence detection system (Applied Biosystems, Foster City, CA). The results were normalized to the β-actin expression (used as endogenous control) and fold-change expression was calculated by using Ct values in comparison with experimental controls that received a value of 1. Primer sequences used were as follows: β-actin, forward primer, 5′-TGT CAC CAA CTG GGA CGA TA-3′, and reverse primer, 5′-AAC ACA GCC TGG ATG GCT AC-3′; iNOS, forward primer, 5′-CAG CGC AGA GGG CTC AAA GG-3′, and reverse primer, 5′-TCG TCG GCC AGC TCT TTC T-3′; TNF-α, forward primer, 5′-ACA AGG CTG CCC CGA CTA T-3′, and reverse primer, 5′-CTC CTG GTA TGA AGT GGC AAA TC-3′; IL-6, forward primer, 5′-GTC AAC TCC ATC TGC CCT TCA G-3′, and reverse primer, 5′-GGC AGT GGC TGT CAA CAA CAT-3′; IL-1β, forward primer, 5′- TAC CTA TGT CTT GCC CGT GGA G-3′, and reverse primer, 5′- ATC ATC CCA CGA GTC ACA GAG G -3′; G-SCF, forward primer, 5′-CAC CTA CAA GCT GTG TCA TCC G-3′, and reverse primer, 5′-AGG CAC TTT GTC TGC CTG CAA G-3′; CD14, forward primer, 5′-CAG GAA CTT TGG CTT TGC TC-3′, and reverse primer, 5′-CCC ATT GAG CCA TCT TGA TT-3′; and myeloid differentiation factor 88 (MyD88), forward primer, 5′-GCG AGC TCA TTG AGA AAA GG-3′, and reverse primer, 5′-CTT GGT GCA AGG GTT GGT AT-3′.

Western blot analysis

Samples were analyzed for protein expression by using standard Western blot techniques. In brief, protein samples were denatured in electrophoresis buffer [50 mM Tris-HCl (pH 6.8), 2% sodium dodecyl sulfate, 10% glycerol, 50 mg/ml bromphenol blue, 2% β-mercaptoethanol] at 95°C for 5 min and subjected to sodium dodecyl sulfate–polyacrylamide gel electrophoresis. Proteins were transferred onto nitrocellulose membranes, and equal loading was confirmed by ponceau-red staining. The membranes were blocked in Tris-buffered saline containing 0.1% Tween 20 (TBS-T) containing 5% nonfat dry milk, 1% BSA (and 1% blocking reagent in the case of iNOS) for 1 h at room temperature. Immunodetection was done by using anti-iNOS antibody (1:500 dilution in TBS-T with 2.5% milk), anti-TLR4 antibody, anti-CD14 antibody, or anti-MyD88 antibody (1:300 dilution in TBS-T with 2.5% milk) at 4°C overnight. After a subsequent washing step, biotin-conjugated anti-rabbit immunoglobulin (for iNOS), peroxidase-conjugated anti-rabbit immunoglobulin (for TLR4), or peroxidase-conjugated anti-goat immunoglobulin (for CD14 and MyD88) was used as a secondary antibody. In the case of iNOS, the membranes were washed and incubated with peroxidase-conjugated streptavidin. Visualization of immunoreactive bands was performed by using ECL detection reagents, and the signal was detected by short exposure to x-ray film. To ensure equal loading of proteins, the blots were stripped and reprobed with anti-β-actin antibody

(1:5,000 dilution in TBS-T with 2.5% milk; 1 h, room temperature), and peroxidase-conjugated anti-mouse immunoglobulin was used as a secondary antibody.

Enzyme-linked immunosorbent assay

The concentrations of cytokines in cell-culture media were determined by using commercially available rat Quantikine enzyme-linked immunosorbent assay (ELISA) kits provided by R&D Systems (Wiesbaden, Germany). All samples were analyzed in triplicate by following instructions of the manufacturer.

Preparation of nuclear extracts

Nuclear extracts were prepared by scraping the cells into extraction buffer (20 m*M* HEPES, pH 7.8, 10 m*M* KCl, 0.1 m*M* EDTA, 1 m*M* dithiotreitol (DTT), and 0.5 m*M* PMSF). Samples were incubated on ice for 15 min, and then 60 μl of 10% NP-40 was added per each 1 ml of extraction buffer. After a quick spin-down, the supernatant was removed, and the pellet was redissolved in extraction buffer containing 400 m*M* NaCl. Samples were incubated on ice with agitation for 15 min, and then centrifuged at 15,000 *g* for 5 min. Supernatants were collected as nuclear extract, and protein concentration was determined by using Bradford reagent with BSA standards.

Electromobility shift assay

NF-κB consensus oligonucleotide was labeled with ^{32}P by using T4 polynucleotide kinase. Five micrograms of nuclear extract and labeled oligonucleotide (10,000 cpm) were used in each reaction. The negative control sample contained no nuclear protein extract. The competition sample contained an equal amount of unlabeled consensus oligonucleotide, used to compete with the labeled probe. For supershift analysis, 2 μl of anti-NF-κB p65 antibody was added. Binding reactions were performed at 4°C overnight in a 2× binding buffer (40 m*M* HEPES, pH 7.5, 50 m*M* NaCl, 1 m*M* EDTA, 1 m*M* DTT, 1 m*M* PMSF, and 1.28 μg/ml competitor DNA). Samples were separated by 4% nondenaturing acrylamide gel electrophoresis in 0.5x TBE buffer at 170 V. After electrophoresis, signal was detected after exposure to developing film at −80°C.

Estimation of intracellular ROS by using dihydroethidium

ROS levels were detected with dihydroethidium (DHE), a redox-sensitive probe, as described previously (1). After the different treatments, KCs were washed with PBS on the plates, and then incubated with 25 μ*M* DHE in 1 ml PBS for 30 min at 37°C. The cells were then scraped, centrifuged, resuspended in PBS, pH 7.4, and fluorescence was detected with flow cytometer (excitation at 488 nm and emission at 575 nm).

Measurement of reduced glutathione

Reduced glutathione (GSH) was measured with high-pressure liquid chromatography (HPLC), as described previously (4), with minor modifications. Samples were prepared by scraping the cells into 1% phosphoric acid and immediate freezing in liquid nitrogen. After thawing, samples were centrifuged at 23,500 *g* for 5 min; supernatants were collected for HPLC analysis, and pellets were used to determine protein amounts. Samples and glutathione standards were run in running buffer (50 m*M* KH_2PO_4 and 2% acetonitrile, pH 2.7) by using a Synergy 4-μm Polar-RP 80A column (Phenomenex, Torrance, CA) when the cell potential was 850 mV. Detection was made with an electrochemical detector. The results were adjusted to protein levels of the samples.

Statistical analysis

Data are expressed as mean ± SEM of independent cell-isolation procedures. Comparisons between two groups were performed with Student's *t* test. Differences with a value of $p = 0.05$ were considered to be significant. Statistical comparisons were performed by using GraphPad Prism 4 software (Graphpad Software, San Diego, CA).

Results

Isolation of KCs and LE treatment

The isolation of KCs from other hepatic nonparenchymal cell populations by counterflow elutriation allows obtaining a high-purity primary KCs culture. The yield was between 50 and 90 million cells/perfused liver with an average viability rate of 97%. Purity of the isolated cells was determined by phase-contrast microscopy and indirect immunofluorescence staining. Cells were stained against ED2 (CD163), a KCs marker (2), and purity was confirmed with 92.3% ED2-positive cells when merged with DAPI nuclear staining (Fig. 1A). Red fluorescence was not detected in negative control-stained cultures, demonstrating specific binding of antibody against ED2 (not shown).

Throughout the experiments, KCs were exposed to LE added to the cell-culture medium as a source of TGs. Thin-layer chromatography (TLC) analysis shows that TGs were not decomposed to FFAs in the medium 6 h after the addition of LE (Fig. 1B).

Nile red staining of the cells was used to detect intracellular lipid droplets. Exposure of KCs to 0.1% TGs for up to 12 h did not result in prominent lipid accumulation, relative to control cells (Fig. 1C, bottom panels). Corresponding phase-contrast images of cultures are also shown (Fig. 1C, top panels), with no evidence of lipotoxicity of TGs at this concentration. Flow cytometry, after annexin-PI staining of LE-exposed cells, verified that exposure to 0.1% TGs was not toxic to the cells up to 48 h (not shown).

Quantitative evaluation revealed no increase in the number of Nile red–positive cells after exposure to LE alone for 2 h and for 6 h. However, an increase in the number of stained cells when adding TGs emulsion to LPS-containing culture media was observed after 2 h. This increase was found to be statistically significant after 6 h of treatment (Fig. 1D).

TGs augment iNOS expression in response to LPS

The induction of iNOS, an established marker of inflammatory activation, was used to study the effect of TGs on this response in KCs.

Treatment of the cells with LPS for 2 h induced marked increase in iNOS mRNA levels. Conversely, TGs alone did not influence iNOS expression. However, simultaneous exposure of the cells to both LPS and TGs resulted in signifi-

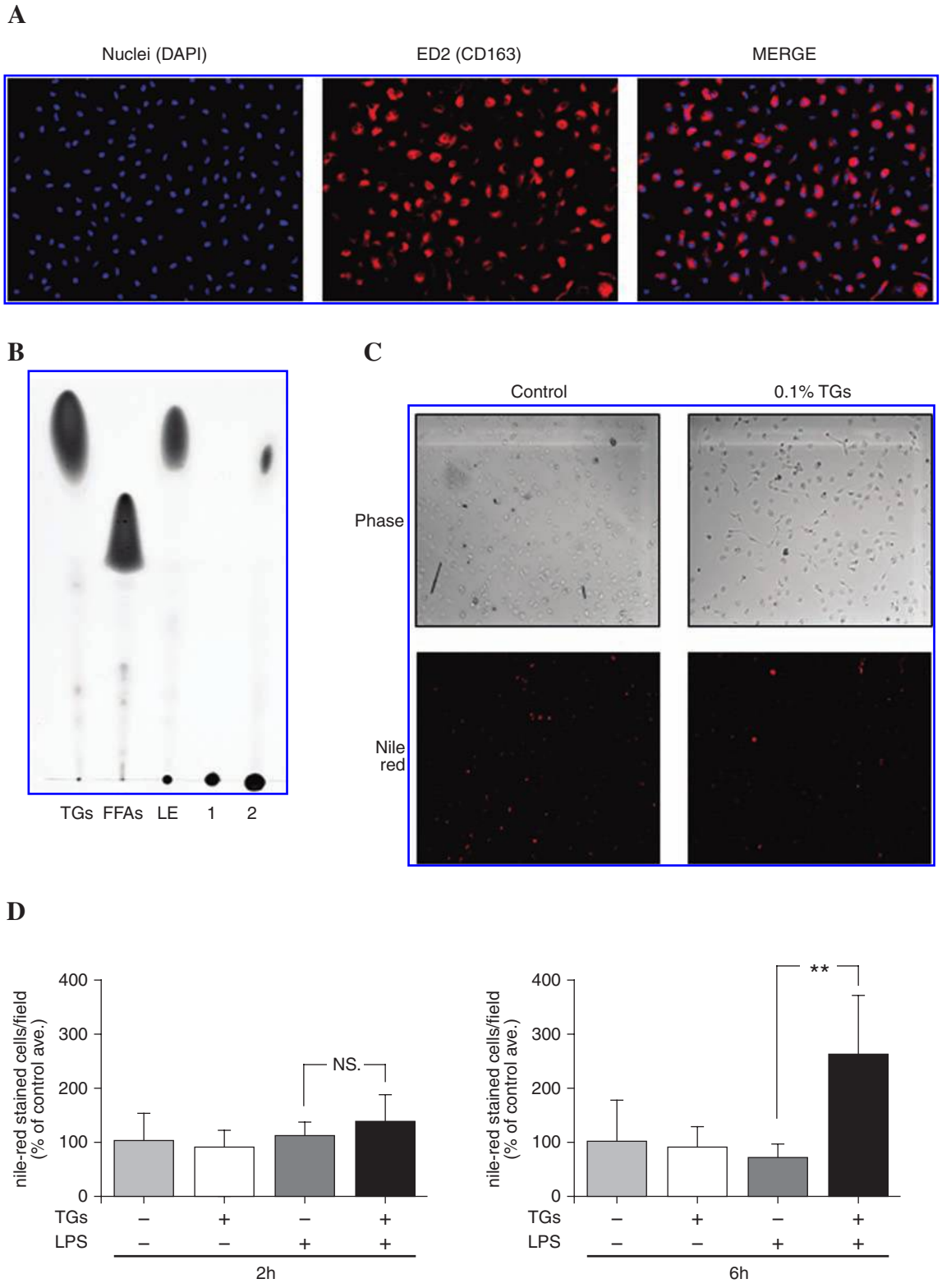

FIG. 1. Isolated KCs cultures, analysis of TGs in the medium, and uptake by the cells. (**A**) Staining KCs cultures against CD163 (ED2) indicates high-purity cultures. DAPI fluorescence image of same field is shown on the left panel. (**B**) As evaluated by TLC compared with standards, no detected FFAs have been seen in the LE and in the cell-culture medium collected from control cells (1) and from cells treated with LE for 6 h (2). (**C**) Nile red staining shows no massive accumulation of lipid droplets in KCs after exposure to TGs for 12 h. Visualization of the same fields as a phase-contrast image is shown in the upper panels. (**D**) Increase in number of Nile red–stained cells is shown after simultaneous exposure to LPS and TGs for 6 h. Positive cells were counted in 10 to 15 different fields for each treatment. Data are presented relative to control treatment average value, which was normalized to a 100 ± SD. N.S., not significant; p (2 h) = 0.12. $^{**}p < 0.01$. (For interpretation of the references to color in this figure legend, the reader is referred to the web version of this article at www.liebertonline.com/ars).

cantly enhanced iNOS induction, compared with only LPS–treated cells (Fig. 2A). iNOS protein expression was not detectable with Western blot analysis in any of the samples at this time point (not shown).

The same effect, of enhanced increase in iNOS mRNA expression, is shown in the cells after 6 h of the combined treatment (Fig. 2A). At the 6-h time point, enhancement is observed also in iNOS protein expression in cells exposed to both LPS and TGs, compared with cells exposed only to LPS (Fig. 2B).

To examine whether the activation of iNOS is affected by the presence of medium-chain TGs (MCTs) found in Lipofundin, its contribution to iNOS induction was compared with that of emulsion containing only LCTs (ClinOleic). LCTs alone were found to enhance the LPS-induced iNOS mRNA expression (Fig. 2C). Further experiments were performed in the presence of lipase inhibitor (Paraoxon). Inhibition of lipase activity did not prevent the TGs-induced increase in iNOS mRNA expression in response to LPS (not shown), indicating that the effect was not mediated by lipase-dependent TGs hydrolysis. Moreover, addition of palmitic acid and linoleic acid (to final concentrations of 10 and 100 μM) together with LPS for 6 h did not induce enhanced iNOS response (Fig. 2D).

TGs increase mRNA expression and secreted levels of cytokines in activated KCs

Because iNOS is a proinflammatory gene, the effect of TGs on proinflammatory cytokines expression was evaluated. TNF-α, IL-1β, and IL-6 are main participants in the activation response of KCs and play a major role in inflammatory processes (2, 5, 38). Expression of all three was induced by adding LPS to the culture medium for 6 h. Like iNOS, the induction of these genes was increased by adding TGs with LPS (Fig. 3A).

G-CSF is a cytokine produced by a variety of immune-system cells, among them macrophages (23), and induces differentiation of granulocytes. G-CSF expression was also strongly induced by LPS in KCs, and its induction was significantly enhanced by simultaneous exposure to TGs and LPS for 2 h or for 6 h (Fig. 3B).

The levels of TNF-α and IL-6 secreted by the cells into culture media were evaluated with ELISA. Increased concentrations of TNF-α and IL-6 are measured after exposure of the cells to LPS for 6 h. The addition of TGs to LPS induced enhancement in the release of both cytokines (Fig. 3C).

TGs effects on LPS-activated KCs are not mediated by increased expression of CD14, MyD88, or TLR4 and do not occur in Zymosan-activated KCs

CD14 acts as a co-receptor of TLR4, the cell-surface receptor responsible for the LPS-responsiveness of the cells (48). Therefore, the effect of TGs treatment on CD14 expression level was evaluated. Exposure to LPS for 6 h, but not for 2 h, increased CD14 mRNA expression. The addition of TGs to LPS-treated cells did not lead to a further increase in CD14 mRNA expression at the 2-h nor at the 6-h time point (Fig. 4A, top).

The expression level of MyD88 was measured in KCs exposed to LPS and TGs. MyD88 is an adaptor molecule for TLR-mediated signaling (5), but its mRNA expression level did not change after treatment of KCs with LPS for 2 h nor for 6 h. MyD88 mRNA expression also was not affected by adding TGs with LPS to the culture medium (Fig. 4A, bottom).

Analysis of TLR4, MyD88, and CD14 at the protein level was performed. According to gene-expression results, the LPS treatment increased CD14 protein expression after 6 h (Fig. 4B), yet no enhancement was seen by adding TGs with LPS. Addition of TGs to LPS did not enhance the protein expression of TLR4 and MyD88 (Fig 4B).

These data indicate that the additive effect of TGs on the KCs activation response is not mediated *via* increased expression of these TLR4 pathway–related molecules.

To verify whether the TGs effect is TLR4 specific, KCs were stimulated with zymosan instead of LPS. Zymosan is a yeast cell-wall polysaccharide that induces proinflammatory cytokines in macrophages by activation of TLR2 signaling (51). KCs express TLR2, yet zymosan induced only small changes in the mRNA-expression level of iNOS in comparison to the increase seen before in response to LPS. Addition of TGs to zymosan for 2 and 6 h did not induce an enhancement in iNOS expression level (Fig. 4C). Likewise, addition of TGs did not enhance the zymosan-induced increase in TNF-α and IL-6 mRNA expression at the 6-h time point (not shown).

Increased NF-κB activation by TGs in activated KCs

The NF-κB transcription factor is involved in the regulation of many proinflammatory mediators (6). Increased DNA-binding activity of NF-κB was seen in nuclear extracts of KCs treated with LPS for 2 h (Fig. 5A). Interestingly, simultaneous treatment with LPS and TGs led to stronger activation of NF-κB (Fig. 5A). Specific binding was demonstrated by cold-probe competition, and the presence of the P65 subunit of NF-κB was confirmed by supershift analysis.

FIG. 2. Effect of TGs and FFAs on iNOS expression in the presence of LPS. (**A**) TGs enhanced the induction of iNOS mRNA expression when added to the culture medium with LPS for 2 or 6 h. $n = 7$; $^*p < 0.05$; $^{**}p < 0.01$. (**B**) *Top*: iNOS protein expression analyzed by Western blot, as shown by a representative gel run of three independent cell-isolation procedures. *Bottom*: The bar graph shows that TGs added to the culture medium together with LPS enhance the expression of iNOS protein, relative to LPS alone. Data are presented relative to the corresponding LPS treatment, which was normalized to 100. (**C**) Comparison between the effect of TGs (Lipofundin emulsion LCTs/MCTs) and only LCT (ClinOleic emulsion) on the expression of iNOS mRNA when added simultaneously with LPS for 2 h (*top*) or 6 h (*bottom*), as presented by a representative experiment of two independent cell-isolation procedures ± SD; $^*p < 0.05$. (**D**) The bar graphs show that addition of palmitic and linoleic acids, in concentration of 10 μM (*top*) and 100 μM (*bottom*), to LPS did not enhance the expression of iNOS protein relative to LPS alone (Dunnett's test). Data are presented relative to the corresponding LPS treatment, which was normalized to 100. Representative gel run of three independent cell-isolation procedures is shown.

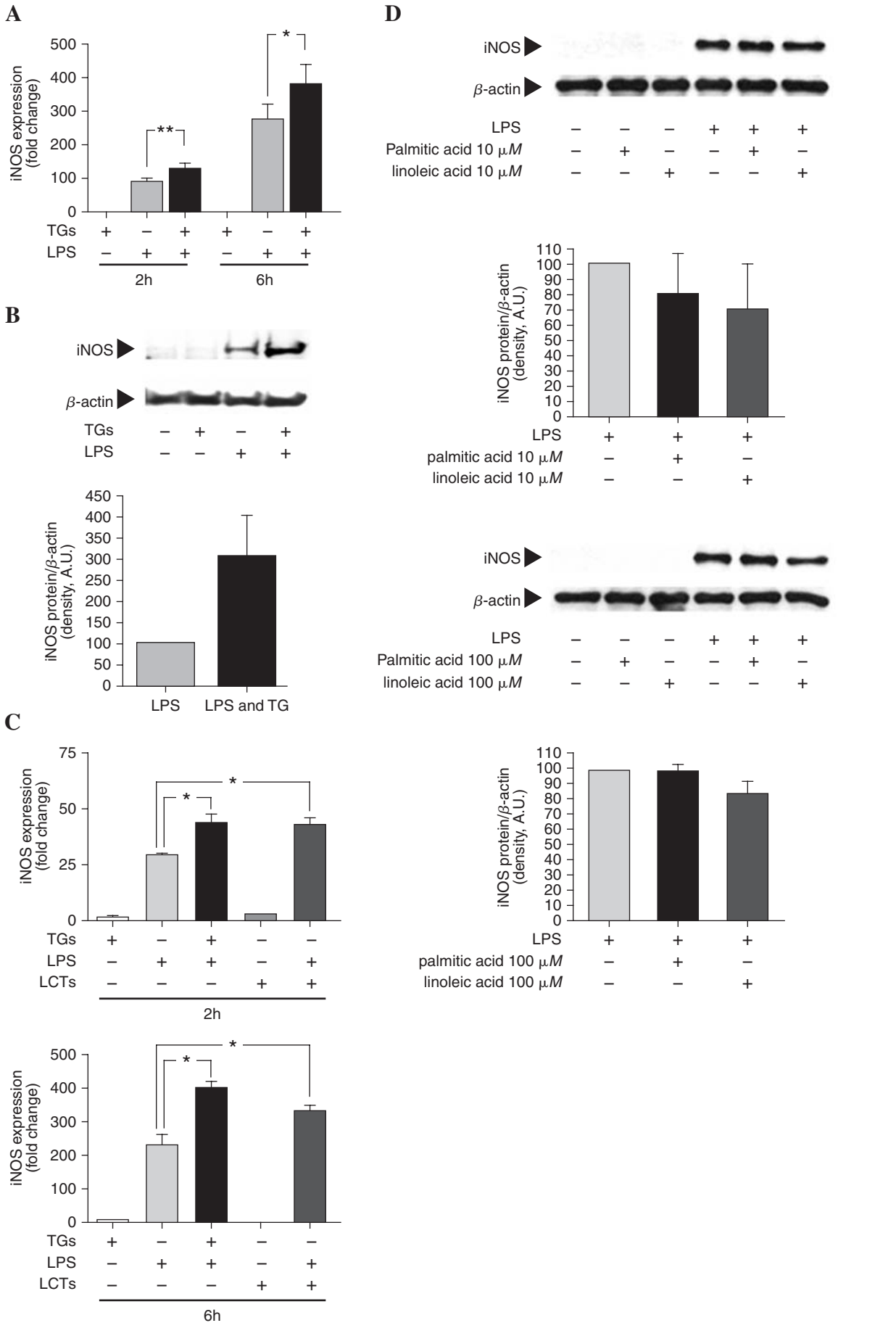
A
iNOS expression (fold change)
500
400
300
200
100
0
*
**
TGs + − + + − +
LPS − + + − + +
2h
6h
B
iNOS
β-actin
TGs − + − +
LPS − − + +
iNOS protein/β-actin (density, A.U.)
450
400
350
300
250
200
150
100
50
0
LPS
LPS and TG
C
iNOS expression (fold change)
75
50
25
0
*
*
TGs + − + − −
LPS − + + − +
LCTs − − − + +
2h
iNOS expression (fold change)
500
400
300
200
100
0
*
*
TGs + − + − −
LPS − + + − +
LCTs − − − + +
6h
D
iNOS
β-actin
LPS − − − + + +
Palmitic acid 10 μM − + − − + −
linoleic acid 10 μM − − + − − +
iNOS protein/β-actin (density, A.U.)
110
100
90
80
70
60
50
40
30
20
10
0
LPS + + +
palmitic acid 10 μM − + −
linoleic acid 10 μM − − +
iNOS
β-actin
LPS − − − + + +
Palmitic acid 100 μM − + − − + −
linoleic acid 100 μM − − + − − +
iNOS protein/β-actin (density, A.U.)
110
100
90
80
70
60
50
40
30
20
10
0
LPS + + +
palmitic acid 100 μM − + −
linoleic acid 100 μM − − +

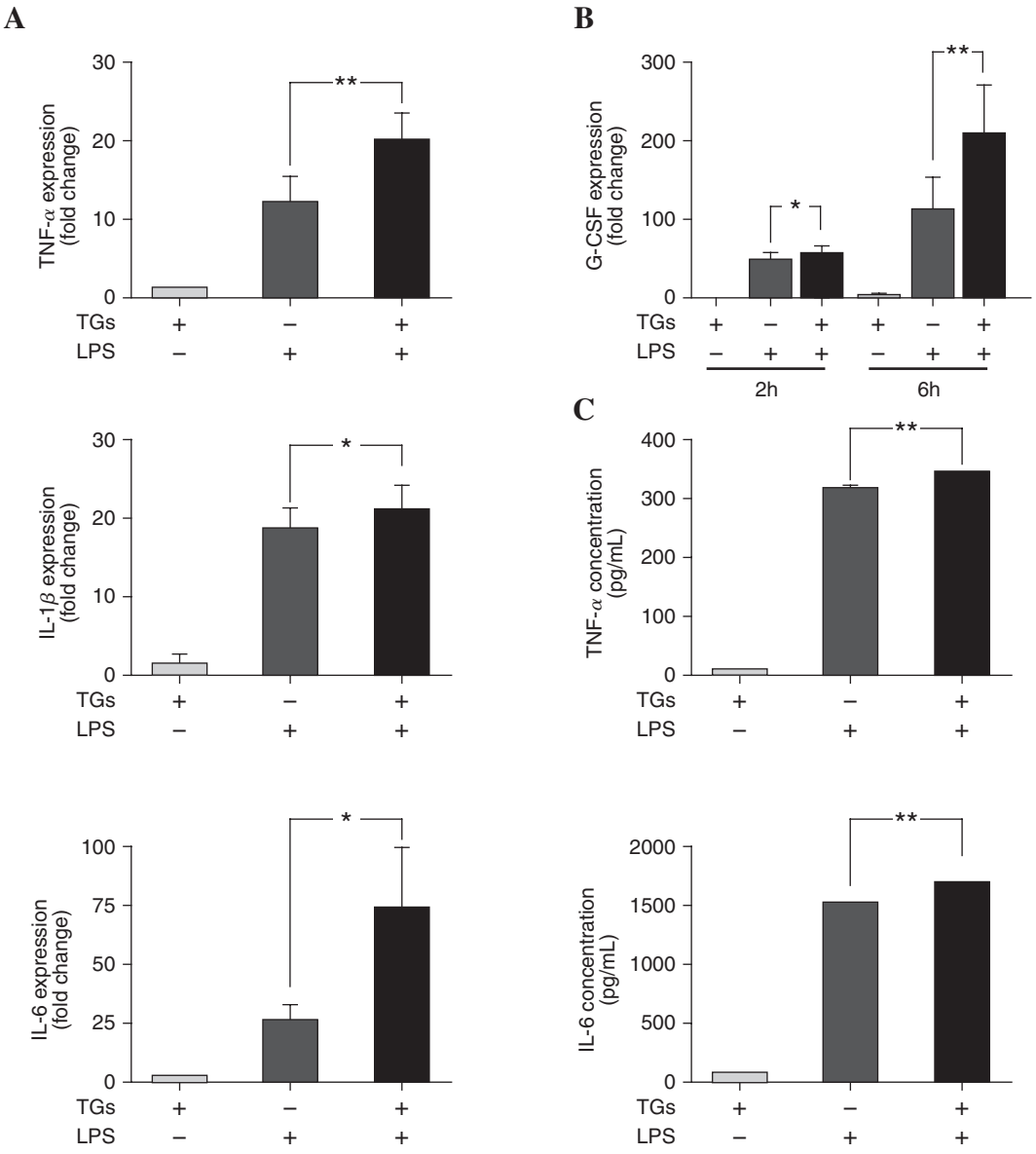

FIG. 3. Effect of TGs on gene expression and secretion of cytokines in activated KCs. (**A**) Simultaneous exposure to TGs and LPS for 6 h synergistically increased the expression level of mRNA of TNF-α (*top*), IL-1β (*middle*), and IL-6 (*bottom*). $n = 7$ for TNF-α and IL-1β, $n = 4$ for IL-6. *$p < 0.05$; **$p < 0.01$. (**B**) Significant enhancement in G-CSF mRNA expression levels is seen when adding TGs to the LPS-containing medium for 2 or 6 h. $n = 7$. *$p < 0.05$; **$p < 0.01$. (**C**) Addition of TGs enhanced the LPS-dependent release of TNF-α (*top*) and IL-6 (*bottom*), as shown in a representative experiment of two independent cell-isolation procedures ± SD; **$p < 0.01$.

To demonstrate that NF-κB activation, which was potentiated by TGs, mediates the observed upregulation of inflammatory genes, NF-κB signaling was suppressed. Pretreatment with Bay 11-7082, an inhibitor of I-κB phosphorylation, abolished the enhanced increase in iNOS protein expression induced by TGs in LPS-activated KCs (Fig. 5B). The inhibitor concentration in our experimental system was calibrated to induce as small effect as possible on the cells treated with LPS alone (Fig. 5B).

TGs decrease ROS levels and increase GSH levels in activated KCs

ROS production is a main event in the activation response of KCs, and NF-κB is known to be a redox-sensitive transcription factor (6, 27). The intracellular levels of ROS were determined by DHE staining and oxidation followed by FACS analysis. Interestingly, TGs appeared to induce a small, yet significant, decrease in ROS levels when added to the culture media with LPS for 2 and 6 h in comparison with treatment with LPS alone (Fig. 6A). A decrease in DHE fluorescence also was seen after exposure to TGs alone, compared with control cells at the 6-h time point (Fig. 6A).

Thiol status was evaluated in the treated cells with HPLC analysis of cellular glutathione. The decrease in ROS levels was accompanied by an elevation in GSH levels in cells exposed to TGs and LPS (Fig. 6B, top). The increase induced in the levels of this antioxidant by the addition of TGs to LPS-treated cells was found to be statistically significant at the 2-h time point. The amount of oxidized glutathione

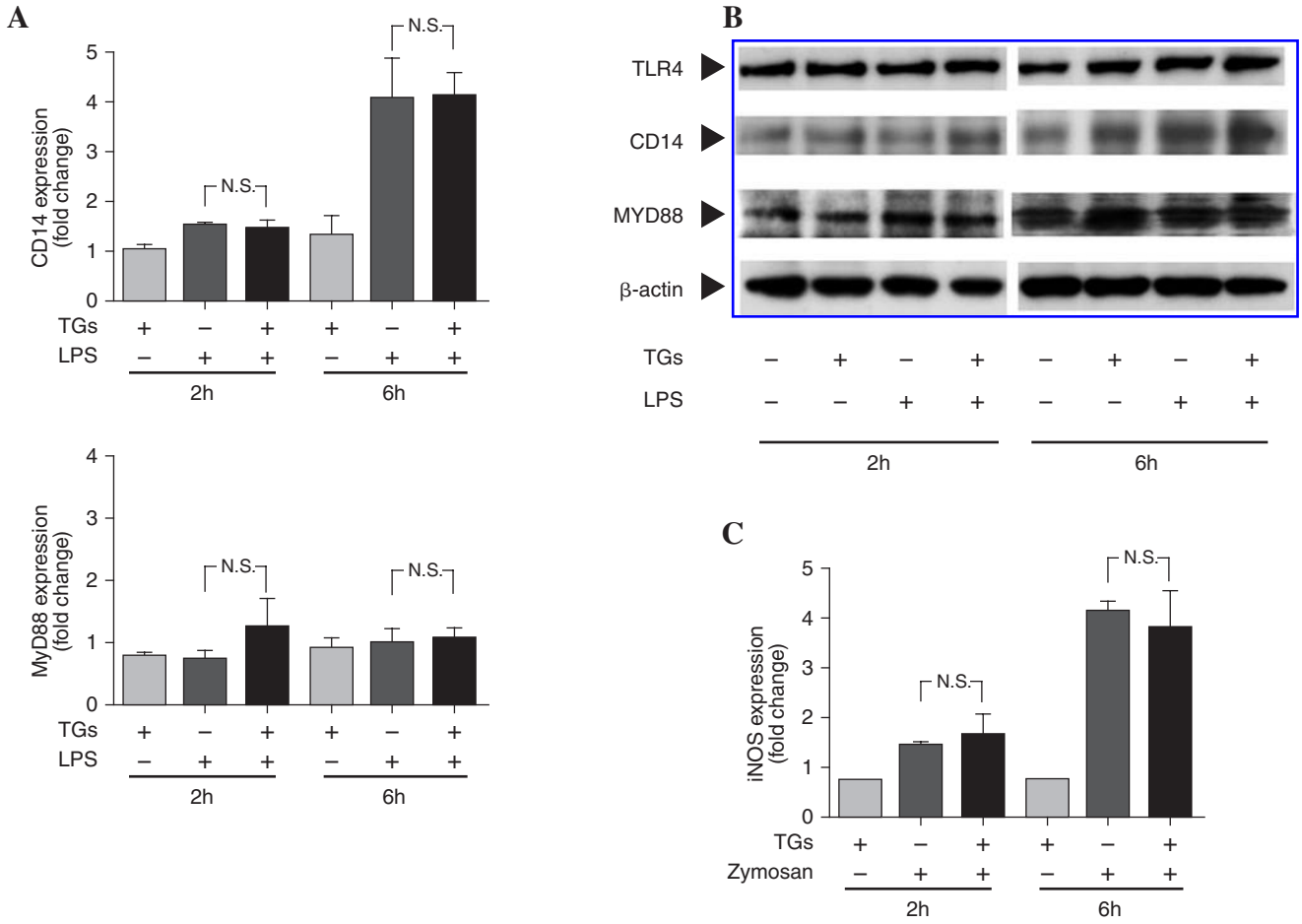

FIG. 4. TLR4, CD14, and MyD88 expression after exposure to LPS or TGs or both and iNOS gene expression after exposure to Zymosan or TGs or both. (**A**) Addition of TGs to the LPS-containing medium for 2 or for 6 h did not change the mRNA expression level of CD14 (*top*) and MyD88 (*bottom*) in the cells. $n = 4$; N.S., not significant; p (2 h) = 0.39, p (6 h) = 0.42 for CD14; p (2 h) = 0.09; p (6 h) = 0.48 for MyD88. (**B**) TLR4 pathway-related molecules protein expression analyzed with Western blot, as shown by a representative gel run. (**C**) Addition of TGs to Zymosan-containing medium did not influence the mRNA expression level of iNOS after 2 or 6 h, as shown by a representative experiment of two independent cell-isolation procedures ± SD; N.S., not significant; p (2 h) = 0.26; p (6 h) = 0.30.

(GSSG) measured in all samples was negligible, as seen in the chromatogram (Fig. 6B, bottom).

Discussion

Several different factors have been suggested to contribute to the process of exacerbation among NAFLD patients and the development of NASH. Those include oxidative stress, release of inflammatory cytokines, and liver cells death (7, 15, 49). We present the potential involvement of KCs in this event under the influence of exposure to TGs. Lipofundin emulsion is used for parenteral nutrition in patients, and liver steatosis is the most common complication of this treatment (22). The uptake of TGs emulsion by cells was studied and was found to be mediated by a coated-pit mechanism (10). An increase in the Nile red–stained KCs number was noticed after combined treatment with LPS. One explanation could be the inhibitory effect of LPS on lipase activity in macrophages (25), which could prevent the decomposition of intracellular TGs.

KCs are main participators in the immune response to bacterial products entering the body, but their function might alter in the setting of liver disease (48). In the fatty-liver environment, KCs are exposed to excess amounts of TGs, which are shown here to increase their responsitivity to endotoxins. Endotoxins are proposed as contributors to NASH development (45), as increased sensitivity to LPS is seen in the murine model of fatty liver (34). Small intestinal bacterial overgrowth is found among NASH patients (52), and treatment with antibiotics or probiotics shows a protective effect (31, 32, 37). Because KCs are the cell type most directly related to the production of inflammatory mediators in the liver (19), their enhanced inflammatory response by TGs might influence the delicate balance between a controlled desirable response and harmful inflammation.

The increased iNOS response shown in our studies might be part of an exaggerated inflammatory response. Other than iNOS, stimulation of KCs triggers the expression of various bioactive molecules. Observations presented herein show that TGs enhanced the LPS-induced increase in the TNF-α, IL-1β, and IL-6 mRNA expression levels, as well as the secretion of TNF-α and IL-6. These mediators are the prototypical proinflammatory cytokines released in different

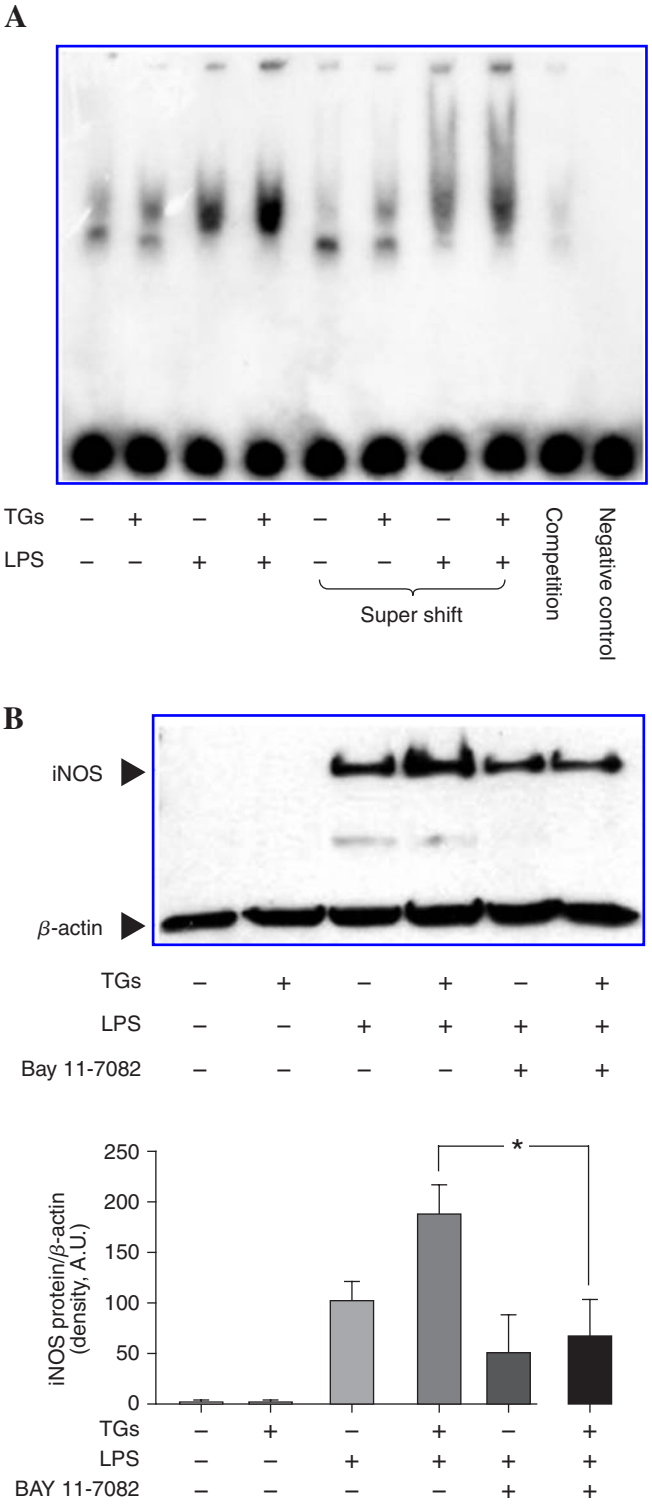

FIG. 5. Involvement of NF-κB activation in response to TGs or LPS treatment or both. (**A**) Activation of NF-κB is induced by LPS and potentiated by simultaneous exposure of cells to LPS and TGs for 2 h. Shown here is a representative EMSA-gel run of three independent cell-isolation procedures. (**B**) *Top*: Western blot analysis of iNOS protein expression, as shown by a representative gel run of three independent cell-isolation procedures. *Bottom*: The bar graph shows that I-κB phosphorylation inhibitor abrogates the enhancement in iNOS protein expression, which is induced by TGs in LPS-activated cells. Data are presented relative to LPS treatment average value, which was normalized to 100. $n = 3$; $^*p < 0.05$.

kinds of liver pathologies (19, 49). TNF-α is the major regulator of liver-disease progression (19, 49). Its critical role in NASH development is emerging in different studies involving both genetic and nutritional rodent models of fatty liver disease (31, 50), as well as from studies revealing enhanced hepatic TNF-α expression among NASH patients, corresponding to disease severity and benefits of treatment with TNF-α inhibitor (15, 42). TNF-α induces other cytokines, such as IL-1 and IL-6 (19, 49), which together act in both autocrine and paracrine fashions regulating the phenotype of neighboring hepatocytes and other nonparenchymal cells and the state of the liver as a whole (5, 19). The exposure to different mixtures of cytokines or endotoxin or both stimulates hepatocytes and endothelial cells, which are also able to release NO during an inflammatory response (11, 18, 21, 28, 41). Increased NO production is also known as an important regulator of blood-vessel permeability, facilitating invasion of immune cells into the inflamed tissue (14). The inflammatory cytokines TNF-α, IL-1β, and IL-6 participate in the recruitment of immune cells into hepatic blood vessels (7, 26, 49). Leukocytic infiltration, which might aggravate the hepatic inflammatory response, is a classic histologic feature of NASH.

Production of G-CSF, strongly induced in macrophages by endotoxin or during bacterial infection, leads to neutrophil chemotaxis (23). The current study indicates enhancement in G-CSF expression in KCs when TGs are added to LPS-containing media. Apart from its role as a growth factor, inducing differentiation of granulocytes, G-CSF also acts as an important immunomodulator, reinforcing the inflammatory response, particularly when it appears adjacent to the inflammatory stimulus (23, 36).

A recent study indicated that TLR4 expression on KCs is a critical component in NASH pathogenesis (40). To elucidate the mechanism of TGs contribution to LPS-mediated KCs inflammatory activation, the expression level of TLR4, CD14, and MyD88 was measured. TLR4 expression was not affected by treatment with LPS and TGs. Together with TLR4, CD14 is responsible for the transmembrane signaling induced by LPS, and downstream, this signaling occurs *via* MyD88 (5). Upregulation in CD14 expression was shown in fatty livers induced in mice by a methionine-choline–deficient (MCD) diet (40, 50), and LPS can enhance CD14 expression in KCs (33). However, according to our results, the addition of TGs does not induce further enhancement in CD14 expression compared with LPS alone, and MyD88 expression was not induced in the cells by adding TGs to LPS. In agreement with that, it was shown previously that TGs emulsion does not change the *in vivo* kinetics of LPS uptake by the liver (39). The lack of effect after Zymosan treatment indicates the importance of the TLR4 pathway in KCs activation in our experimental setting. Therefore, the TGs potentiating effect should be explained by the activation of intracellular events downstream to the TLR4 signaling pathway, which are probably affected by redox changes.

Next, the activation of the transcription factor NF-κB, a key mediator of the cellular inflammatory responses, was investigated. As seen by the EMSA results, LPS treatment induced increased NF-κB activation in isolated KCs. This response was clearly enhanced when co-exposing the cells to TGs and LPS, indicating a stronger inflammatory activation by this combination. NF-κB activation is induced downstream of TLR4 and plays an eminent role in induction of various proinflammatory

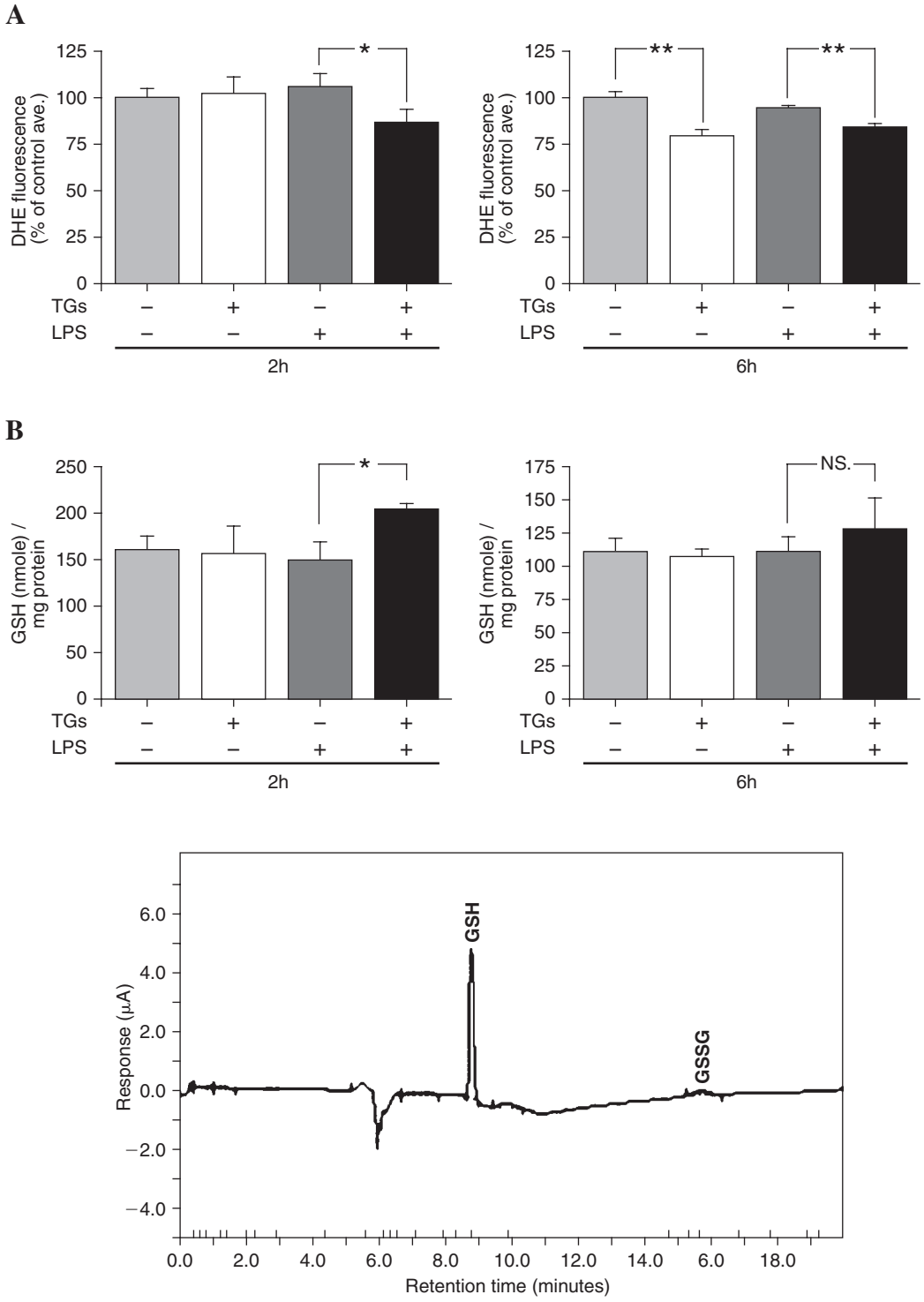

FIG. 6. Intracellular ROS and GSH levels after exposure to TGs or LPS or both. (**A**) TGs decreased ROS levels in the cells when added to culture media in addition to LPS for 2 or for 6 h or alone for 6 h. Data presented relative to control treatment average fluorescence value, which was normalized to 100 ± SD. Treatments were performed in triplicate. $*p < 0.05$; $**p < 0.01$. (**B**) *Top*: TGs increased GSH levels when added to LPS-activated cells. GSH amounts are normalized to protein levels. Treatments were performed in triplicate and are presented as mean ± SD; N.S., not significant. $**p < 0.01$; p (6 h) = 0.12. *Bottom*: A representative HPLC chromatogram. Peaks of glutathione in reduced form (GSH) and oxidized form (GSSG) are indicated.

genes, among them, iNOS, TNF-α, IL-1β, IL-6, and G-CSF (6, 17). It is shown here that the inhibition of NF-κB by Bay 11-7082 efficiently counteracts the added effect of TGs on LPS-induced iNOS protein expression. This observation indicates the involvement of increased NF-κB activation, which can be induced by released cytokines (6).

Fatty acids are capable of activating TLR4-dependent inflammatory signaling in macrophages (44). A direct influ-

ence of different fatty acids on iNOS expression and NO production in response to endotoxin has been previously demonstrated to involve NF-κB activation in a macrophage cell line (16). We found that TGs augment the iNOS response and NF-κB activity in activated KCs, but increased iNOS response did not appear after the addition of palmitic acid and linoleic acid to activated KCs. The TGs effect on iNOS expression was also observed in the presence of lipase inhibitor. Together, these data imply that the potentiation effect seen in our experiments is mediated by TGs, and not by FFAs released from the TGs.

Finally, exposure to TGs seemed to decrease ROS production and to increase GSH levels in LPS-activated cells. Increased capacity to maintain glutathione in the reduced form is seen in activated KCs and may play an important role in the protection against ROS (46). GSH was also shown to support NO production and to be required for full iNOS activity in macrophages (47). Upregulation of GSH levels is a typical stress response of cells. This may be the implication of fat accumulation in KCs. Evidence connecting endogenous ROS production to inhibition, rather then induction of NF-κB activation, is reported (24). A possible explanation of our observations is that decreased oxidative conditions in LPS-activated cells are facilitated by TGs. This may create a reductive environment that is favorable for NF-κB DNA binding, although LPS stimulus is obligatory for this pathway activation.

Much remains to be learned about the mechanistic basis of the interaction between lipids and KCs in NAFLD. Although accumulation of TGs in the liver results in hepatic steatosis, it is also an essential component of the hepatic regeneration process *in vivo*. Therefore, steatosis is part of a designed protective response in the liver (9). Likewise, addition of soybean oil emulsion to a parenteral nutrition regimen prevented the hepatic dysfunction associated with this intervention in infant rats (35). It has been shown that TGs themselves are not hepatotoxic in MCD diet–induced steatohepatitis in mice (53). In this model, TGs synthesis actually helps to protect liver cells from lipotoxicity by buffering the accumulation of FFAs.

Herein it was demonstrated that TGs can induce overactivation of KCs and enhance the release of NO and cytokines. This activation may contribute to amplification of the inflammatory response, which might lead eventually to the development of NASH. Therefore, it is important to elucidate the possible contribution of TGs to these processes.

Acknowledgments

The first two authors contributed equally to this work. This study was supported by a grant of the Ministry of Science and Culture of Niedersachsen to O.T. Z.M. and G.R., and by grant 377/06 from the ISF to O.T. and Z.M. This work also was supported by grants of the Deutsch Forschungsgemeinschaft SFB 402 TP C6, D3, D4. We also thank the Center of Diabetes Research of the Hebrew University of Jerusalem for their support with a scholarship to N.B. The authors wish to thank Miss Sandra Georgi for excellent technical assistance.

Abbreviations

DAPI, 4′,6-diamidino-2-phenylindole; DHE, dihydroethidium; ELISA, enzyme-linked immunosorbent assay; EMSA, electromobility-shift assay; FFAs, free fatty acids; GI, gastrointestinal; G-CSF, granulocyte colony-stimulating factor; GSH, reduced glutathione; HPLC, high-performance liquid chromatography; IL-1β, interleukin-1-beta; IL-6, interleukin-6; iNOS, inducible nitric oxide synthase; KCs, Kupffer cells; LCTs, long-chain triglycerides; LE, lipid emulsion; LPS, lipopolysaccharide; MCTs, medium-chain triglycerides; MyD88, myeloid differentiation factor 88; NAFLD, nonalcoholic fatty-liver disease; NASH, nonalcoholic steatohepatitis; NF-κB, nuclear factor κB; NO, nitric oxide; PBS, phosphate-buffered saline; ROS, reactive oxygen species; TGs, triglycerides; TLC, thin-layer chromatography; TLR, Toll-like receptor; TNF-α, tumor necrosis factor-alpha.

References

1. Aharoni-Simon M, Reifen R, and Tirosh O. ROS-production-mediated activation of AP-1 but not NFkappaB inhibits glutamate-induced HT4 neuronal cell death. *Antioxid Redox Signal* 8: 1339–1349, 2006.
2. Armbrust T and Ramadori G. Functional characterization of two different Kupffer cell populations of normal rat liver. *J Hepatol* 25: 518–528, 1996.
3. Armbrust T, Schwogler S, Zohrens G, and Ramadori G. C1 esterase inhibitor gene expression in rat Kupffer cells, peritoneal macrophages and blood monocytes: modulation by interferon gamma. *J Exp Med* 178: 373–380, 1993.
4. Aronis A, Madar Z, and Tirosh O. Mechanism underlying oxidative stress-mediated lipotoxicity: exposure of J774.2 macrophages to triacylglycerols facilitates mitochondrial reactive oxygen species production and cellular necrosis. *Free Radic Biol Med* 38: 1221–1230, 2005.
5. Bilzer M, Roggel F, and Gerbes AL. Role of Kupffer cells in host defense and liver disease. *Liver Int* 26: 1175–1186, 2006.
6. Blackwell TS and Christman JW. The role of nuclear factor-kappa B in cytokine gene regulation. *Am J Respir Cell Mol Biol* 17: 3–9, 1997.
7. Browning JD and Horton JD. Molecular mediators of hepatic steatosis and liver injury. *J Clin Invest* 114: 147–152, 2004.
8. Calder PC, Bond JA, Harvey DJ, Gordon S, and Newsholme EA. Uptake and incorporation of saturated and unsaturated fatty acids into macrophage lipids and their effect upon macrophage adhesion and phagocytosis. *Biochem J* 269: 807–814, 1990.
9. Canbay A, Bechmann L, and Gerken G. Lipid metabolism in the liver. *Z Gastroenterol* 45: 35–41, 2007.
10. Carvalho MD, Harada LM, Gidlund M, Ketelhuth DF, Boschcov P, and Quintao EC. Macrophages take up triacylglycerol-rich emulsions at a faster rate upon co-incubation with native and modified LDL: an investigation on the role of natural chylomicrons in atherosclerosis. *J Cell Biochem* 84: 309–323, 2002.
11. Ceppi ED, Smith FS, and Titheradge MA. Effect of multiple cytokines plus bacterial endotoxin on glucose and nitric oxide production by cultured hepatocytes. *Biochem J* 317: 503–507, 1996.
12. Chaet MS, Garcia VF, Arya G, and Ziegler MM. Dietary fish oil enhances macrophage production of nitric oxide. *J Surg Res* 57: 65–68, 1994.
13. Chakravortty D and Hensel M. Inducible nitric oxide synthase and control of intracellular bacterial pathogens. *Microbes Infect* 5: 621–627, 2003.
14. Cirino G, Fiorucci S, and Sessa WC. Endothelial nitric oxide synthase: the Cinderella of inflammation? *Trends Pharmacol Sci* 24: 91–95, 2003.

15. Crespo J, Cayon A, Fernandez-Gil P, Hernandez-Guerra M, Mayorga M, Dominguez-Diez A, Fernandez-Escalante JC, and Pons-Romero F. Gene expression of tumor necrosis factor alpha and TNF-receptors, p55 and p75, in nonalcoholic steatohepatitis patients. *Hepatology* 34: 1158–1163, 2001.
16. de Lima TM, de Sa Lima L, Scavone C, and Curi R. Fatty acid control of nitric oxide production by macrophages. *FEBS Lett* 580: 3287–3295, 2006.
17. Ding WX and Yin XM. Dissection of the multiple mechanisms of TNF-alpha-induced apoptosis in liver injury. *J Cell Mol Med* 8: 445–454, 2004.
18. Feder LS and Laskin DL. Regulation of hepatic endothelial cell and macrophage proliferation and nitric oxide production by GM-CSF, M-CSF, and IL-1 beta following acute endotoxemia. *J Leukoc Biol* 55: 507–513, 1994.
19. Ferre N and Claria J. New insights into the regulation of liver inflammation and oxidative stress. *Mini Rev Med Chem* 6: 1321–1330, 2006.
20. Fowler SD and Greenspan P. Application of Nile red, a fluorescent hydrophobic probe, for the detection of neutral lipid deposits in tissue sections: comparison with oil red O. *J Histochem Cytochem* 33: 833–836, 1985.
21. Geller DA, Nussler AK, Di Silvio M, Lowenstein CJ, Shapiro RA, Wang SC, Simmons RL, and Billiar TR. Cytokines, endotoxin, and glucocorticoids regulate the expression of inducible nitric oxide synthase in hepatocytes. *Proc Natl Acad Sci U S A* 90: 522–526, 1993.
22. Guglielmi FW, Boggio-Bertinet D, Federico A, Forte GB, Guglielmi A, Loguercio C, Mazzuoli S, Merli M, Palmo A, Panella C, Pironi L, and Francavilla A. Total parenteral nutrition-related gastroenterological complications. *Dig Liver Dis* 38: 623–642, 2006.
23. Hareng L and Hartung T. Induction and regulation of endogenous granulocyte colony-stimulating factor formation. *Biol Chem* 383: 1501–1517, 2002.
24. Hayakawa M, Miyashita H, Sakamoto I, Kitagawa M, Tanaka H, Yasuda H, Karin M, and Kikugawa K. Evidence that reactive oxygen species do not mediate NF-kappaB activation. *EMBO J* 22: 3356–3366, 2003.
25. Hill MR, Kelly K, Wu X, Wanker F, Bass H, Morgan C, Wang C, and Gimble JM. Lipopolysaccharide regulation of lipoprotein lipase expression in murine macrophages. *Infect Immun* 63: 858–864, 1995.
26. Jaeschke H. Mechanisms of liver injury, II: Mechanisms of neutrophil-induced liver cell injury during hepatic ischemia-reperfusion and other acute inflammatory conditions. *Am J Physiol Gastrointest Liver Physiol* 290: G1083–G1088, 2006.
27. Janssen YM and Sen CK. Nuclear factor kappa B activity in response to oxidants and antioxidants. *Methods Enzymol* 300: 363–374, 1999.
28. Kitade H, Sakitani K, Inoue K, Masu Y, Kawada N, Hiramatsu Y, Kamiyama Y, Okumura T, and Ito S. Interleukin 1 beta markedly stimulates nitric oxide formation in the absence of other cytokines or lipopolysaccharide in primary cultured rat hepatocytes but not in Kupffer cells. *Hepatology* 23: 797–802, 1996.
29. Knook DL and Sleyster EC. Separation of Kupffer and endothelial cells of the rat liver by centrifugal elutriation. *Exp Cell Res* 99: 444–449, 1976.
30. Laskin JD, Heck DE, Gardner CR, and Laskin DL. Prooxidant and antioxidant functions of nitric oxide in liver toxicity. *Antioxid Redox Signal* 3: 261–271, 2001.
31. Li Z, Yang S, Lin H, Huang J, Watkins PA, Moser AB, Desimone C, Song XY, and Diehl AM. Probiotics and antibodies to TNF inhibit inflammatory activity and improve nonalcoholic fatty liver disease. *Hepatology* 37: 343–350, 2003.
32. Loguercio C, De Simone T, Federico A, Terracciano F, Tuccillo C, Di Chicco M, and Carteni M. Gut-liver axis: a new point of attack to treat chronic liver damage? *Am J Gastroenterol* 97: 2144–2146, 2002.
33. Matsuura K, Ishida T, Setoguchi M, Higuchi Y, Akizuki S, and Yamamoto S. Upregulation of mouse CD14 expression in Kupffer cells by lipopolysaccharide. *J Exp Med* 179: 1671–1676, 1994.
34. Nolan JP and Vilayat M. Endotoxin and the liver, I: Toxicity in rats with choline deficient fatty livers. *Proc Soc Exp Biol Med* 129: 29–31, 1968.
35. Oshita M, Takehara H, Yamaguchi M, Doi K, Ueda N, Naito S, Hiraoka I, and Tashiro S. Significance of administration of fat emulsion: hepatic changes in infant rats receiving total parenteral nutrition with and without fat. *Clin Nutr* 23: 1060–1068, 2004.
36. Pajkrt D, Manten A, van der Poll T, Tiel-van Buul MM, Jansen J, Wouter ten Cate J, and van Deventer SJ. Modulation of cytokine release and neutrophil function by granulocyte colony-stimulating factor during endotoxemia in humans. *Blood* 90: 1415–1424, 1997.
37. Pappo I, Bercovier H, Berry EM, Haviv Y, Gallily R, and Freund HR. Polymyxin B reduces total parenteral nutrition-associated hepatic steatosis by its antibacterial activity and by blocking deleterious effects of lipopolysaccharide. *J Parenter Enteral Nutr* 16: 529–532, 1992.
38. Ramadori G and Saile B. Inflammation, damage repair, immune cells, and liver fibrosis: specific or nonspecific, this is the question. *Gastroenterology* 127: 997– 1000, 2004.
39. Rensen PC, Oosten M, Bilt E, Eck M, Kuiper J, and Berkel TJ. Human recombinant apolipoprotein E redirects lipopolysaccharide from Kupffer cells to liver parenchymal cells in rats in vivo. *J Clin Invest* 99: 2438–2445, 1997.
40. Rivera CA, Adegboyega P, van Rooijen N, Tagalicud A, Allman M, and Wallace M. Toll-like receptor-4 signaling and Kupffer cells play pivotal roles in the pathogenesis of nonalcoholic steatohepatitis. *J Hepatol* 47: 571–579, 2007.
41. Rockey DC and Chung JJ. Regulation of inducible nitric oxide synthase in hepatic sinusoidal endothelial cells. *Am J Physiol* 271: G260–G267, 1996.
42. Satapathy SK, Sakhuja P, Malhotra V, Sharma BC, and Sarin SK. Beneficial effects of pentoxifylline on hepatic steatosis, fibrosis and necroinflammation in patients with non-alcoholic steatohepatitis. *J Gastroenterol Hepatol* 22: 634–638, 2007.
43. Schaffer JE. Lipotoxicity: when tissues overeat. *Curr Opin Lipidol* 14: 281–287, 2003.
44. Shi H, Kokoeva MV, Inouye K, Tzameli I, Yin H, and Flier JS. TLR4 links innate immunity and fatty acid-induced insulin resistance. *J Clin Invest* 116: 3015–3025, 2006.
45. Solga SF and Diehl AM. Non-alcoholic fatty liver disease: lumen-liver interactions and possible role for probiotics. *J Hepatol* 38: 681–687, 2003.
46. Spolarics Z and Wu JX. Role of glutathione and catalase in H2O2 detoxification in LPS-activated hepatic endothelial and Kupffer cells. *Am J Physiol* 273: G1304–G1311, 1997.
47. Stuehr DJ, Kwon NS, and Nathan CF. FAD and GSH participate in macrophage synthesis of nitric oxide. *Biochem Biophys Res Commun* 168: 558–565, 1990.
48. Su GL. Lipopolysaccharides in liver injury: molecular mechanisms of Kupffer cell activation. *Am J Physiol Gastrointest Liver Physiol* 283: G256–G265, 2002.

49. Tilg H and Hotamisligil GS. Nonalcoholic fatty liver disease: cytokine-adipokine interplay and regulation of insulin resistance. *Gastroenterology* 131: 934–945, 2006.
50. Tomita K, Tamiya G, Ando S, Ohsumi K, Chiyo T, Mizutani A, Kitamura N, Toda K, Kaneko T, Horie Y, Han JY, Kato S, Shimoda M, Oike Y, Tomizawa M, Makino S, Ohkura T, Saito H, Kumagai N, Nagata H, Ishii H, and Hibi T. Tumour necrosis factor alpha signalling through activation of Kupffer cells plays an essential role in liver fibrosis of non-alcoholic steatohepatitis in mice. *Gut* 55: 415–424, 2006.
51. Wetzler LM. The role of Toll-like receptor 2 in microbial disease and immunity. *Vaccine* 21(suppl 2): S55–S60, 2003.
52. Wigg AJ, Roberts-Thomson IC, Dymock RB, McCarthy PJ, Grose RH, and Cummins AG. The role of small intestinal bacterial overgrowth, intestinal permeability, endotoxaemia, and tumour necrosis factor alpha in the pathogenesis of non-alcoholic steatohepatitis. *Gut* 48: 206–211, 2001.
53. Yamaguchi K, Yang L, McCall S, Huang J, Yu XX, Pandey SK, Bhanot S, Monia BP, Li YX, and Diehl AM. Inhibiting triglyceride synthesis improves hepatic steatosis but exacerbates liver damage and fibrosis in obese mice with nonalcoholic steatohepatitis. *Hepatology* 45: 1366–1374, 2007.

Address reprint requests to:
Oren Tirosh
The School of Nutritional Sciences
Institute of Biochemistry, Food Science and Nutrition
Faculty of Agricultural, Food and
Environmental Quality Sciences
The Hebrew University of Jerusalem, Israel

E-mail: otirosh@agri.huji.ac.il

Date of first submission to ARS Central, August 12, 2007; date of final revised submission, June 10, 2008; date of acceptance, June 10, 2008.

This article has been cited by:

1. Naila Naz, Ihtzaz A Malik, Nadeem Sheikh, Shakil Ahmad, Sajjad Khan, Martina Blaschke, Frank Schultze, Giuliano Ramadori. 2012. Ferroportin-1 is a ‘nuclear’-negative acute-phase protein in rat liver: a comparison with other iron-transport proteins. *Laboratory Investigation* **92**:6, 842-856. [CrossRef]
2. Noga Budick-Harmelin, Sarit Anavi, Zecharia Madar, Oren Tirosh. 2012. Fatty acids-stress attenuates gluconeogenesis induction and glucose production in primary hepatocytes. *Lipids in Health and Disease* **11**:1, 66. [CrossRef]
3. Ihtzaz Ahmed Malik, Naila Naz, Nadeem Sheikh, Sajjad Khan, Federico Moriconi, Martina Blaschke, Giuliano Ramadori. 2011. Comparison of changes in gene expression of transferrin receptor-1 and other iron-regulatory proteins in rat liver and brain during acute-phase response. *Cell and Tissue Research* **344**:2, 299-312. [CrossRef]
4. Edna Meilin, Michael Aviram, Tony Hayek. 2011. Insulin increases macrophage triglyceride accumulation under diabetic conditions through the down regulation of hormone sensitive lipase and adipose triglyceride lipase. *BioFactors* **37**:2, 95-103. [CrossRef]
5. Noriko Yamabe, Jeong Sook Noh, Chan Hum Park, Ki Sung Kang, Naotoshi Shibahara, Takashi Tanaka, Takako Yokozawa. 2010. Evaluation of loganin, iridoid glycoside from Corni Fructus, on hepatic and renal glucolipotoxicity and inflammation in type 2 diabetic db/db mice. *European Journal of Pharmacology* **648**:1-3, 179-187. [CrossRef]
6. Christian J. Steib, Manfred Bilzer, Mark op den Winkel, Susanne Pfeiler, Anna C. Hartmann, Martin Hennenberg, Burkhard Göke, Alexander L. Gerbes. 2010. Treatment with the leukotriene inhibitor montelukast for 10 days attenuates portal hypertension in rat liver cirrhosis. *Hepatology* **51**:6, 2086-2096. [CrossRef]
7. Xavier Prieur, Tamás R#szer, Mercedes Ricote. 2010. Lipotoxicity in macrophages: evidence from diseases associated with the metabolic syndrome. *Biochimica et Biophysica Acta (BBA) - Molecular and Cell Biology of Lipids* **1801**:3, 327-337. [CrossRef]
8. Pan Gao, Liang-Yi Si. 2010. Meprin-# metalloproteases enhance lipopolysaccharide-stimulated production of tumour necrosis factor-# and interleukin-1# in peripheral blood mononuclear cells via activation of NF-#B. *Regulatory Peptides* **160**:1-3, 99-105. [CrossRef]
9. Jörn M. Schattenberg, Marcus Schuchmann. 2009. Diabetes and apoptosis: liver. *Apoptosis* **14**:12, 1459-1471. [CrossRef]